

ASPEN-HYSYS Simulation of an Adiabatic Multi-Packed Bed Reactor with Inter-Stage Quenching for Methanol Synthesis

Sidi-Yacoub Ilhem*, **Feddag Ahmed**, Abdelhamid Ibn Badis University, Mostaganem, Algeria; and **Khelifa Ikram**, GL3Z Gas Liquefaction Complex, Sonatrach Arzew, Algeria

Abstract

The aim of this study was to design a simple and user-friendly model for simulating the adiabatic multiphase fixed-bed reactor utilized in methanol synthesis at the Methanol and Synthetic Resins Complex in Arzew, Algeria. The process was based on the ICI (Imperial Chemical Industries) method, employing a copper oxide-based catalyst (CuO, ZnO, or Al₂O₃). Methanol is synthesized from syngas, which is a mixture of CO, CO₂, and H₂, and acts as the primary feedstock for methanol production in this reactor setup.

The developed model provides the capability to predict methanol yield, control high temperatures resulting from exothermic reactions within each catalyst bed, and determine the necessary amount of quenching gas injection to reduce the temperature. Through simulations, we achieved a crude methanol ratio of 3.41, closely matching the estimated ratio of 3.4 in the actual reactor. This outcome serves as strong evidence for the effectiveness of the designed model in simulating complex chemical reactors.

Building on these promising results, the study proceeded to the recycling simulation stage, where the mass of crude methanol was increased to 4.1%. This step indicates the model's capacity to handle and optimize the recycling process, which is crucial for enhancing the overall efficiency and sustainability of methanol production in the complex. By accurately predicting process parameters and performance, the developed model proves to be a valuable tool for advancing methanol synthesis technologies and promoting more efficient industrial practices.

Introduction

Fixed-bed, multi-stage adiabatic reactors are commonly used in the chemical and petrochemical industries due to their cost-effectiveness in terms of operation and maintenance (Cui and Kær 2020). These reactors consist of a vertical cylindrical vessel that contains multiple layers of catalyst arranged in series. The catalyst beds are vertically stacked, resembling a large cylindrical column (Bendjaouahdou and Bendjaouahdou 2014). Each bed consists of compact and fixed catalyst particles, as shown in **Figure 1**. These reactors are primarily employed for heterogeneous and exothermic chemical reactions, and they are equipped with a cooling system to maintain a consistent temperature and prevent catalyst damage.

Various cooling techniques can be employed, including the quenching method. This method involves injecting a cold gas between the catalyst beds to mix with the hot gas generated from the exothermic reactions, thus lowering the temperature of the mixture before it enters the subsequent catalyst bed.

Effective temperature control is crucial for this approach. The temperature resulting from the chemical reactions in each catalyst bed needs to be determined in order to calculate the amount of cold gas required to control the temperature of the gas mixture.

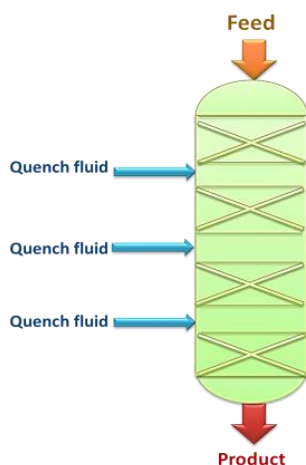


Figure 1—Multi-bed reactor with quenching systems.

Numerical simulations have become a rapid and efficient method for predicting and controlling fixed-bed reactors and their associated cooling systems. The main goal of this study was to develop a user-friendly and practical model to simulate a multi-stage adiabatic reactor used in methanol synthesis within the Arzew industrial area. The model was designed to facilitate temperature control and predict methanol production rates in each catalytic bed. For this purpose, we opted for the renowned Aspen-HYSYS V11 software, known for its excellence in designing, controlling, and optimizing industrial processes. This software provides a wide range of unit operations and accurately determines solid catalyst properties and kinetics of heterogeneous chemical reactions (Adeniyi et al. 2018).

Furthermore, the software allows for easy transition from batch to continuous mode by incorporating gas recycling functionality. This flexibility provides enhanced process control and efficiency.

We started by presenting the methanol synthesis reactor in the CP1Z complex of the Arzew refinery, located in the industrial area of the El Mahgoune plateau, 2 kilometers from the city of Arzew and about 40 kilometers from the city of Oran.

The methanol synthesis follows the ICI (Imperial Chemical Industries) process and was conducted in an adiabatic catalytic reactor. The reactor was designed as a vertical cylindrical vessel and consists of four catalyst beds arranged in series. Each catalytic stage comprises a tightly packed and stationary arrangement of catalyst particles.

During the reaction, temperatures range from approximately 210°C to 270°C, and the pressure is maintained at 52 bar (Ortiz et al. 2013). The exothermic nature of the reaction generates heat, which needs to be effectively managed to maintain optimal operating conditions.

To control the temperature and remove excess heat, cold synthesis gas, also known as quench gas, is injected between the catalyst layers (Lee 1989). The quench gas serves the purpose of cooling the reaction mixture. This injection of cold gas helps regulate and maintain the desired temperature levels within the reactor.

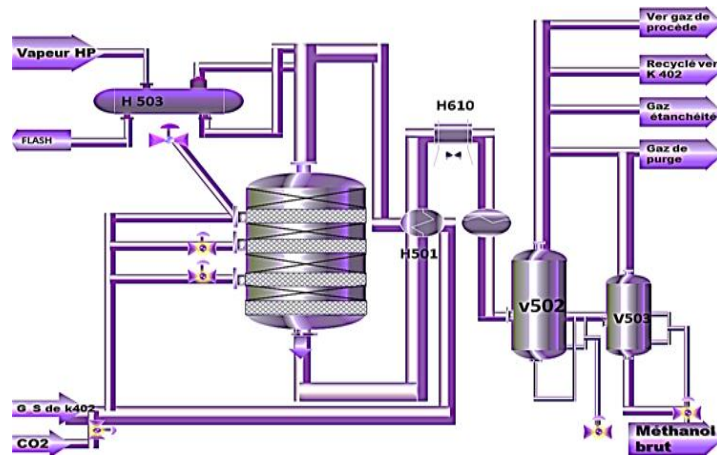


Figure 2—Methanol synthesis reactor at the level of the CP1Z complex of Arzew.

Modeling Approach

Fluid Package. In this study, the Peng-Robinson equation of state was employed to calculate the thermodynamic properties of the reaction mixture. The Peng-Robinson equation is known for its accurate estimation of vapor pressure and fluid density. One of its advantages is that it requires minimal experimental data and allows for a concise simulation period (Slattery 1972).

The Peng-Robinson equation is defined by the coefficients ‘a’ and ‘b’, which are determined by the following relationships:

$$p = \frac{RT}{v-b} - \frac{a}{v^2 + 2bv - b^2}, \dots\dots\dots (1)$$

$$b = 0.0778 \frac{R^2 T_c^2}{P_c}, \dots\dots\dots (2)$$

$$a(T) = 0.45724 \frac{R^2 T_c^2}{P_c} \alpha(T), \dots\dots\dots (3)$$

$$\alpha^{0.5} = 1 + m(1 - T_r^{0.5}), \dots\dots\dots (4)$$

$$m = 0.37464 + 1.54226\omega - 0.26992\omega^2, \dots\dots\dots (5)$$

$$T_r = \frac{T}{T_c}, \dots\dots\dots (6)$$

The Peng-Robinson equation provides an effective framework for accurately modeling the thermodynamic behavior of the reaction mixture in the methanol synthesis process.

Kinetic Theory of Methanol Synthesis. Methanol is synthesized from a mixture of CO, CO₂, and H₂ gases, typically using a commercial Cu/ZnO/Al₂O₃ catalyst (Blumberg et al. 2017; Fuad et al. 2012). This catalyst enables the production of methanol under relatively ‘mild’ conditions (210-270 °C and 50-100 bar), as depicted in the equations presented in **Table 1**.

Table 1—Reaction Formulas for Methanol Synthesis (Graaf et al. 1990; Moulijn et al. 2013)

Reaction	Reaction enthalpy
(1) CO + H ₂ O ↔ CO ₂ + H ₂	-41 (kJ/mol)
(2) CO ₂ + 3H ₂ ↔ CH ₃ OH + H ₂ O	-49.67 (kJ/mol)
(3) CO + 2H ₂ ↔ CH ₃ OH	-90.64 (kJ/mol)

In the literature, various kinetic models have been employed to describe the kinetics of methanol synthesis (Skrzypek et al. 1995). Bussche and Froment (1996) and Løvik (2001) conducted comprehensive evaluations of multiple processes investigated, each with its unique constraints.

The behavior of kinetic laws is influenced by factors such as the catalyst type, the composition of the feed gas, and the reaction conditions (temperature and pressure). While some models assume that the synthesis gas comprises CO and H₂, others allow for the presence of CO₂ in the feed.

In the past, producers believed that methanol synthesis relied solely on the hydrogenation of carbon monoxide (CO). Consequently, they removed all carbon dioxide (CO₂) from the feed gas through absorption (Fossen et al. 2022). However, experiments conducted by Waugh (2012) demonstrated that the presence of carbon dioxide in the gas mixture actually accelerates the methanol production process compared to feed gas containing only H₂ and CO (Abate et al. 2015).

In our study, we employed the kinetic theory developed by Bussche and Forment (1996) along with the equilibrium constants derived from the equations proposed by Graaf et al (1990). This widely applicable theory has been experimentally validated, and adjustments have been made to its parameters by Bussche and Forment (1996) to enhance its suitability across various cases.

The results of numerous experiments conducted by different researchers (Nestler et al. 2018) indicate that methanol synthesis predominantly occurs through the hydrogenation of carbon dioxide rather than carbon monoxide. It is crucial to consider the water-gas shift (WGS) reaction when describing the methanol synthesis process (Bussche and Froment 1996). Therefore, before converting carbon monoxide into methanol, it must undergo the water-gas shift reaction to produce carbon dioxide(Goeppert et al. 2014; Shi et al. 2020).



Our study focuses on two key reactions: the water-gas shift (WGS) transformation reaction and the hydrogenation of carbon dioxide, which yield methanol (Bozzano and Manenti 2016).

Reaction 1: $\text{CO} + \text{H}_2\text{O} \leftrightarrow \text{CO}_2 + \text{H}_2$

$$r_1 = \frac{k_e p_{\text{CO}_2} \left(1 - K_2^{eq} \left(\frac{p_{\text{H}_2\text{O}} p_{\text{CO}}}{p_{\text{H}_2} p_{\text{CO}_2}} \right) \right)}{1 + \frac{k_c p_{\text{H}_2\text{O}}}{p_{\text{H}_2}} + k_a \sqrt{p_{\text{H}_2}} + k_b p_{\text{H}_2\text{O}}}, \dots \dots \dots (8)$$

Reaction 2: $\text{CO}_2 + 3\text{H}_2 \leftrightarrow \text{CH}_3\text{OH} + \text{H}_2\text{O}$

$$r_2 = \frac{k_d p_{\text{CO}_2} p_{\text{H}_2} \left(1 - \left(\frac{1}{K_1^{eq}} \right) \left(\frac{p_{\text{H}_2\text{O}} p_{\text{CH}_3\text{OH}}}{p_{\text{H}_2} p_{\text{CO}_2}^3} \right) \right)}{\left(1 + \frac{k_c p_{\text{H}_2\text{O}}}{p_{\text{H}_2}} + k_a \sqrt{p_{\text{H}_2}} + k_b p_{\text{H}_2\text{O}} \right)^3}, \dots \dots \dots (9)$$

The values and initial reactions associated with the adsorption equilibrium constants as presented in Eq. 8 and 9, are illustrated in **Figure 1** and detailed in **Table 2**. As shown in Table 2, the kinetics of reactions 1 and 2 are expressed in terms of pressure and reaction rate.

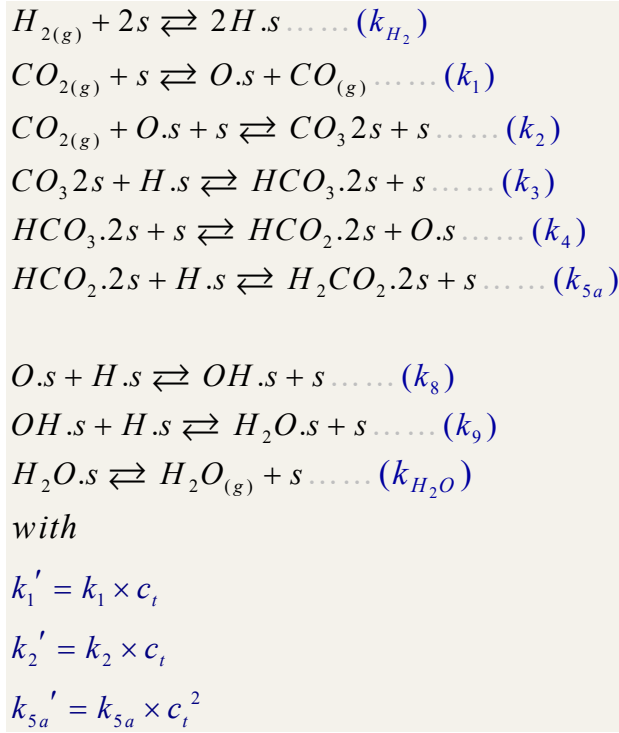


Figure 3—Initial reactions associated with the adsorption equilibrium

Table 2—Kinetic constants of reactions 1 and 2.

$k = A e^{(B/RT)}$	Units	A	B
$\sqrt{k_{H_2}}$	bar ^{-1/2}	0.499	17197
k_{H_2O}	bar ⁻¹	6.62e ⁻¹¹	124119
$(k_{H_2O} / k_8 k_9 k_{H_2})$	mol/kg s bar ²	3453.38	-
$(k_{5a}' k_2' k_3 k_4 k_{H_2})$	-	1.07	36696
k_1'	mol/kg s bar	1.22e ⁻¹	-9476

Table 3—Equilibrium constants from the Graaf's equation (Graaf et al. 1986)

$\log_{10}(K_1^{eq}) = \frac{3066}{T} - 10,592$	bar ⁻²
$\log_{10}(K_2^{eq}) = \frac{-2073}{T} - 2,029$	dimensionless

The Langmuir-Hinshelwood-Hougen-Watson (LHHW) type integral equation, obtained from the kinetics and parameters developed by Bussche and Forment (1996), is employed by ASPEN-HYSYS to describe the methanol production kinetics (Tripodi et al. 2017). This model accurately depicts the characteristics of both methanol production reactions. The LHHW kinetic model comprises a kinetic factor, a driving force expression, and an adsorption term (Al-Malah 2022).

$$r = (\text{kinetic_factor}) \frac{(\text{driving_force})}{(\text{adsorption_term})} \dots\dots\dots(10)$$

To incorporate the kinetic equation into the Aspen HYSYS model, the units must be modified and changed from kilograms of catalyst to moles per volume of the gas phase.

$$r = \left[\frac{\text{mol}}{\text{s kgcat}} \right] \rightarrow r \times \rho_c \frac{(1-\varphi)}{\varphi} \rightarrow r_{\text{HYSYS}} = \left[\frac{\text{mol}}{\text{s m}_{\text{gas}}^3} \right], \dots \dots \dots (11)$$

The two reactions' rate expressions have been modified to:

$$r_1 = \frac{3,5 \cdot 10^{10} \exp\left(\frac{-94765}{RT}\right) p_{\text{CO}_2} - 3,28 \cdot 10^8 \exp\left(\frac{-55080}{RT}\right) p_{\text{H}_2\text{O}} p_{\text{CO}} p_{\text{H}_2}^{-1}}{1 + 3453,4 p_{\text{H}_2\text{O}} p_{\text{H}_2}^{-1} + 0,499 \exp\left(\frac{17197}{RT}\right) P_{\text{H}_2}^{0,5} + 6,62 \cdot 10^{-11} \exp\left(\frac{124119}{RT}\right) p_{\text{H}_2\text{O}}}, \dots \dots \dots (12)$$

$$r_2 = \frac{3,08 \cdot \exp\left(\frac{36696}{RT}\right) p_{\text{CO}_2} p_{\text{H}_2} - 1,204 \cdot 10^{11} \exp\left(\frac{-21999}{RT}\right) p_{\text{H}_2\text{O}} p_{\text{CH}_3\text{OH}} p_{\text{H}_2}^{-2}}{\left(1 + 3453,4 p_{\text{H}_2\text{O}} p_{\text{H}_2}^{-1} + 0,499 \exp\left(\frac{17197}{RT}\right) P_{\text{H}_2}^{0,5} + 6,62 \cdot 10^{-11} \exp\left(\frac{124119}{RT}\right) p_{\text{H}_2\text{O}}\right)^3}, \dots \dots \dots (13)$$

Modeling of the Fixed-bed Adiabatic Reactor. Several studies have been conducted on the modeling of heterogeneous fixed-bed catalytic reactors, including Deasch and Frument (1971), Frument (1972), and Varma (1981). Froment (1972) proposed the most commonly used categorization of fixed-bed reactor models, which can be classified into two main categories: pseudo-homogeneous models and heterogeneous models.

Heterogeneous models take into account fast reactions and significant thermal effects, requiring differentiation between fluid conditions at the surface and inside the catalyst particles. On the other hand, pseudo-homogeneous models assume that the entire catalyst surface is exposed to fluid conditions, treating the reactor as a single-phase system. Froment's (1972) classification divides these models into six categories, consisting of three types of pseudo-homogeneous models and three types of heterogeneous models (Elnashaie 1994).

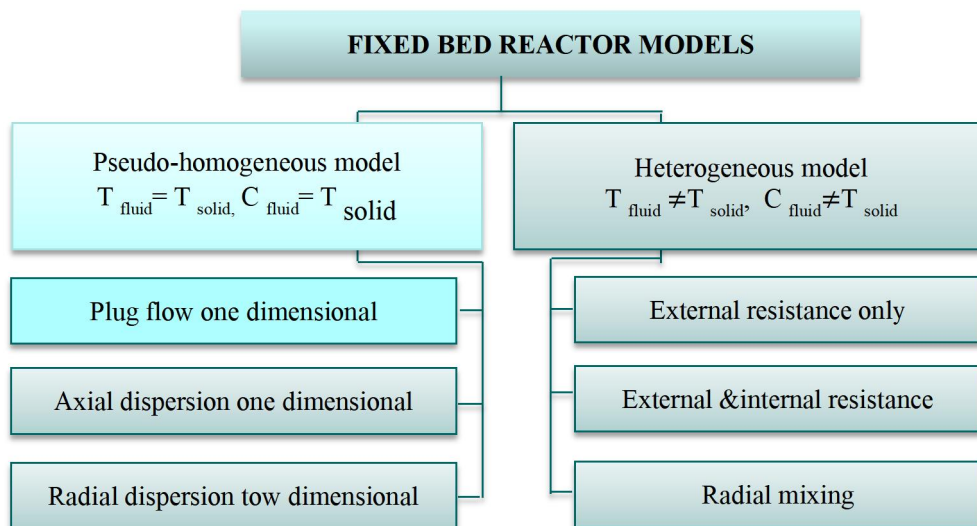


Figure 4—Forment's classification of fixed bed reactor models.

According to the Forment classification of fixed-bed reactor models shown in **Figure 4**, the one-dimensional plug flow reactor (PFR) model is the simplest of the pseudo-homogeneous models. We utilized the PFR reactor available in the ASPEN-HYSYS program library, which represents a tubular reactor assuming perfect radial mixing and zero axial dispersion (Towler and Sinnott 2022). Choosing the

PFR-HYSYS model enables us to incorporate the type of heterogeneous catalyst reaction using the LHHW (Langmuir-Hinshelwood-Hougen-Watson) formula.

Additionally, PFR-HYSYS offers an optional energy stream for heat storage or dissipation. In the absence of flow, HYSYS assumes that the reactor operates as an adiabatic system (HYSYS 2004), which corresponds to a fixed-bed adiabatic reactor for methanol synthesis. The PFR-HYSYS model represents a tubular reactor divided into subvolumes based on the total length and calculated throughout the entire PFR. The default number of subvolumes is 20, but it can be reduced to a minimum (HYSYS, 2004). Therefore, we reduced the number of sections to one in order to simulate a methanol reactor with a single cylindrical vessel.

For simulating the catalyst beds in the methanol reactor, we modeled each catalytic bed using a PFR-HYSYS reactor with a diameter equal to that of the original methanol production reactor and a height equal to the height of each catalytic layer, as illustrated in **Figure 5**.

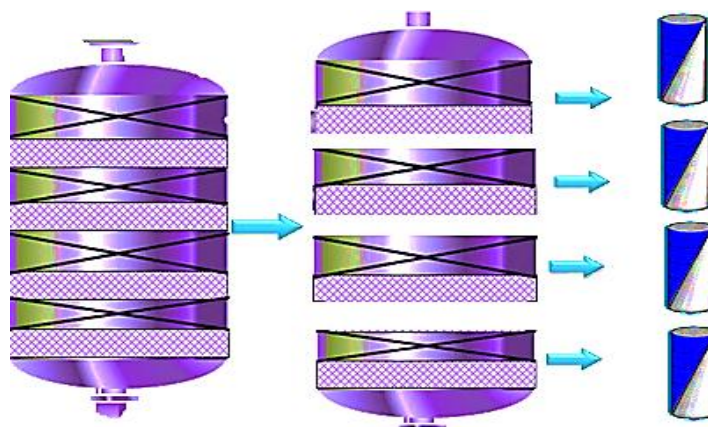


Figure 5—Representation of catalyst layers using four PFR reactors.

Aspen HYSYS offers the benefit of solving each installation component separately instead of attempting to solve them all at once (Liu and Karimi 2018). This capability enables solving the first bed by utilizing a small PFR-HYSYS model, followed by the second, third, and fourth beds in consecutive order.

Pressure Drop. The pressure drops across fixed beds are calculated directly by the ASPEN HYSYS software using the Ergun equation (Grabow and Mavrikakis 2011; Sinadinovic-Fiser et al. 2001).

$$\frac{dP}{dZ} = -\frac{G}{\rho g_c D_p} \left(\frac{1-\phi}{\phi^3} \right) \left[\frac{150(1-\phi)\mu}{D_p} + 1.75G \right], \dots\dots\dots(14)$$

By incorporating the Ergun equation and considering these parameters, the ASPEN HYSYS software accurately calculates the pressure drops in fixed beds. **Tables 4** through **6** provide technical information on the reactor utilized in the simulation. The molar fractions of the gaseous mixture at the inlet of the Arzew reactor are presented in **Table 7**.

Table 4—Operating conditions of the reactor.

Parameters	Value
Reactor inlet flow rate (kmol/h)	14220
First catalytic bed flow rate (kmol/h)	9960
Quench gas flow rate (kmol/h)	4260
Inlet pressure (atm)	52
Inlet temperature (°C)	230
Quench gas temperature (°C)	70

Table 5—Characteristics of the reactor.

Parameters	Value
Number of catalytic beds	4
Height of each catalytic beds (m)	0.75
Reactor diameter (m)	3.9
Void fraction	0.38

Table 6—Catalyst characteristics.

Parameters	Value
Solid density (kg/m ³ -solide)	1770
Particle diameter (mm)	5.4

Table 7—Molar composition of the synthesis gas.

Feed composition	Molar fraction
CO	7.5 %
CO ₂	6 %
H ₂	73.7 %
H ₂ O	0.13 %
N ₂	3.26 %
CH ₄	9.36 %
CH ₃ OH	0

Process Simulation

The synthesis gas, at a pressure of 52 bars and a temperature of 70°C, is divided into two streams. The first stream is preheated to 230°C in a tubular heat exchanger by exchanging heat with the effluent from the reactor, and this stream is used as the feed for the reactor. The second stream, at a temperature of 70°C, acts as a quench gas to cool the reactants. The gaseous reaction mixture flows through the four catalytic stages from top to bottom, as illustrated in **Figure 6**.

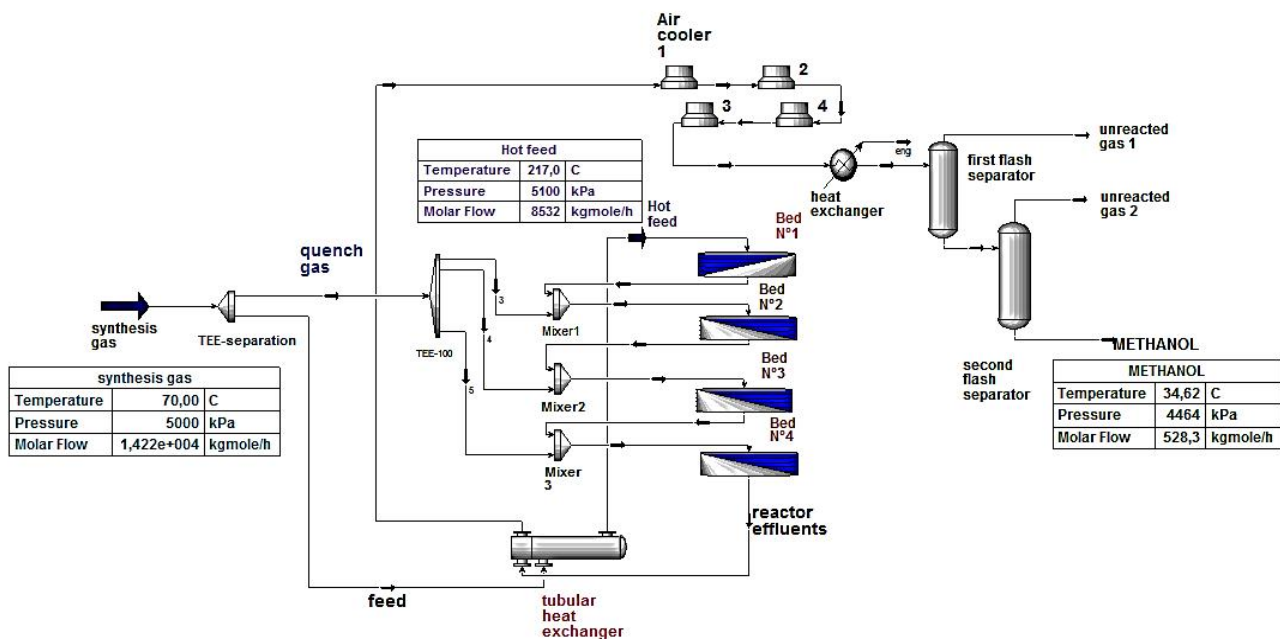


Figure 6—Flowsheet of the methanol process designed in Aspen HYSYS.

Due to the highly exothermic nature of both chemical reactions, it is crucial to cool the reaction mixture by introducing cold synthesis gas between the catalyst layers. This cooling operation is achieved by mixing the gas exiting each bed with a flow of quench gas in a mixer to maintain the temperature within the range of 230°C to 270°C.

The gas leaving the reactor is then cooled to 130°C in a tubular heat exchanger, further cooled to 50°C using air-cooled heat exchangers, and finally cooled to 35°C using another heat exchanger that utilizes cooling water. The cooled gas is separated in the first flash separator to recover the crude methanol and any unreacted gas. To enhance the purity of the final product, a second flash separator is added at the liquid outlet of the first flash separator.

Temperature Control. The primary aim of this endeavor is to effectively monitor and regulate temperature fluctuations occurring within the catalyst. As a result, we present the meticulous findings acquired during this simulation, which are comprehensively summarized in **Table 8**.

Table 8—Temperature and Gas Mixture Flow Rate for Each of the Four Beds.

Catalytic bed	Catalytic bed inlet		Catalytic bed outlet		Quench	
	Flow (K mole/h)	Temperature (K°)	Flow (K mole/h)	Temperature (K°)	Flow (K mole/h)	Temperature (K°)
1	8532	217	8532	263,3	1706	70
2	9919	231,3	9919	255.6	1991	70
3	11740	225 .5	11740	249.9	1991	70
4	13330	224.7	13330	245.9		

Table 8 presents temperature readings at the inlet and outlet of each catalytic layer, along with the required flow rate of cold gas to be injected between consecutive catalyst beds. For example, in the first catalytic bed, the gas mixture temperature increased from 217 °C to 263 °C. Before proceeding to the next stage, we injected 1706 mol/h of refrigerant gas at 70 °C to cool the mixture down to 231 °C. We followed the same procedure for Layers 3 and 4.

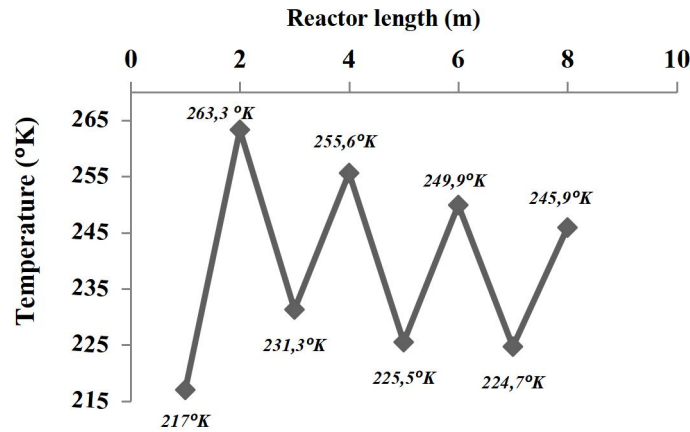


Figure 7—Evaluation of Methanol Synthesis Temperature along the Catalytic Reactor.

Based on the results summarized in Table 8 and Figure 7, we concluded that simulating the reactor in this manner provides a clear understanding of the temperature variation of the gas mixture passing through the four catalyst layers, which is useful for controlling and studying temperature changes.

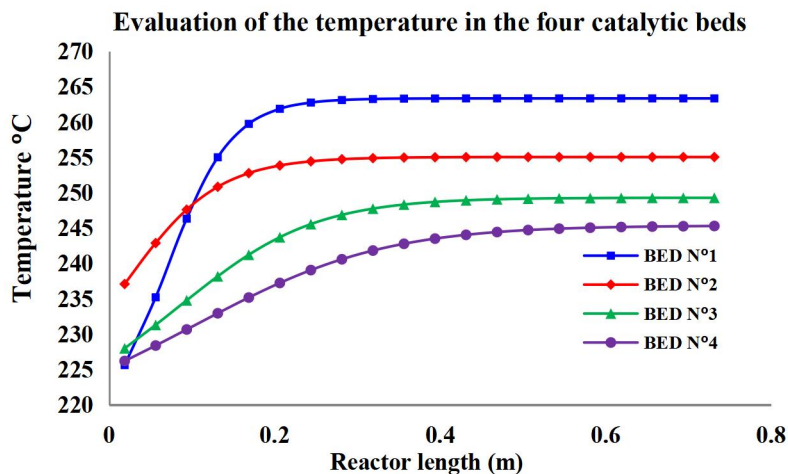


Figure 8—Evaluation of the Synthesis Temperature of Methanol in the Four Catalytic Layers.

Additionally, it allows us to determine the amount of refrigerant gas needed to be injected at the inlet of each stage in order to lower the temperature. The temperature profiles for the four beds exhibit an increasing trend due to the exothermic nature of the two reaction. According to Figures 7 and 8, we observed that the temperature gradient along the first bed is higher compared to the other three beds. This can be attributed to high concentration of reactants (CO and CO₂) and low content of methanol in the initial feed flow rate.

Component Conversion. The component molar fraction ratios for the four catalytic layers are shown in Table 9 for the gas mixture.

Table 9—Molar Fraction of the Reaction Mixture in Each Catalytic Bed.

Composition	Mole fraction (%)							
	First catalyst bed		Second catalyst bed		Third catalyst bed		Fourth catalyst bed	
	Inlet	Outlet	Inlet	Outlet	Inlet	Outlet	Inlet	Outlet
CO	7.5	6.66	6.78	6.15	6.36	5.72	5.96	5.4
CO ₂	6	7.31	7.43	7.44	7.53	7.54	7.60	7.6
H ₂	73.7	70.07	70.42	69.8	70.20	69.55	69.93	69.35
H ₂ O	0.13	1.12	0.9	1.08	0.91	1.06	0.93	1.06
Methanol	0	2	1.6	2.56	2.13	3.04	2,6	3.41

A noticeable shift in the molar percentages of all compounds is clearly observed between the inlet and outlet of each layer within the reactor. For instance, at the outlet of the initial catalytic bed, the concentration of methanol is measured at 2%. Subsequent to the introduction of a precise quantity of refrigerant gas, the molar fraction decreases to 1.6%. Subsequently, the methanol concentration increases to 2.5% at the outlet of the second bed and further rises to 3.04% at the outlet of the third bed. Finally, the methanol concentration reaches 3.41%

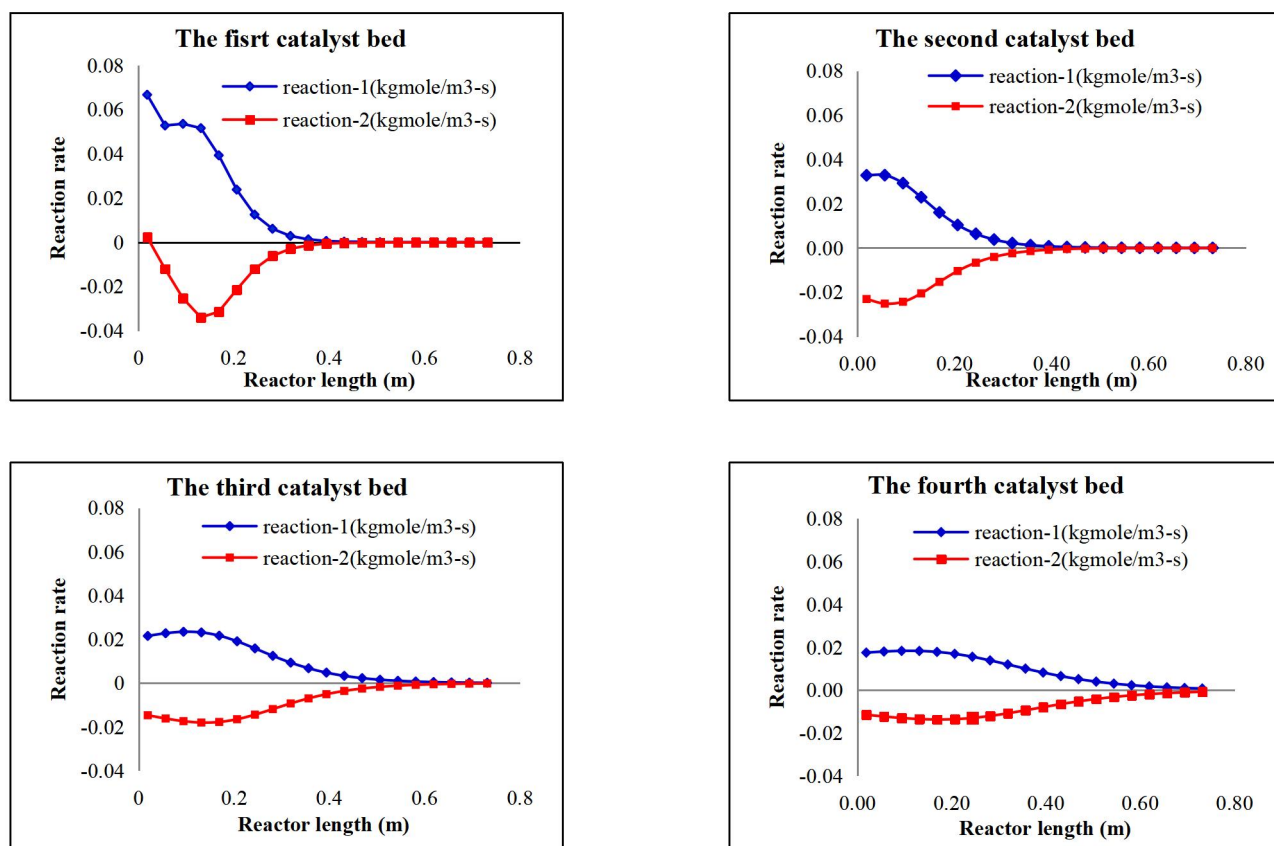


Figure 9—Reactions rate along the catalytic beds.

As observed in **Figure 9**, the rate of the methanol synthesis reaction initially decreased before stabilizing, while the water-gas shift reaction (WGS) increased, resulting in the production of CO₂. Both reactions occur

simultaneously until reaching equilibrium after 50% of the bed length. Since CO_2 is consumed by the methanol synthesis reaction, and also produced by the water-gas shift reaction, CO and H_2O combine to form CO_2 , which then reacts with H_2 to produce methanol.

This is evident from the gradual decrease in the concentrations of CO and CO_2 , accompanied by an increase in the concentration of methanol, as the reaction progresses through each layer, as shown in **Figure 10**. The slight increase in the mole fractions of the reactants (CO and CO_2) at the inlet of each bed can be explained by the introduction of fresh syngas (quench gas).

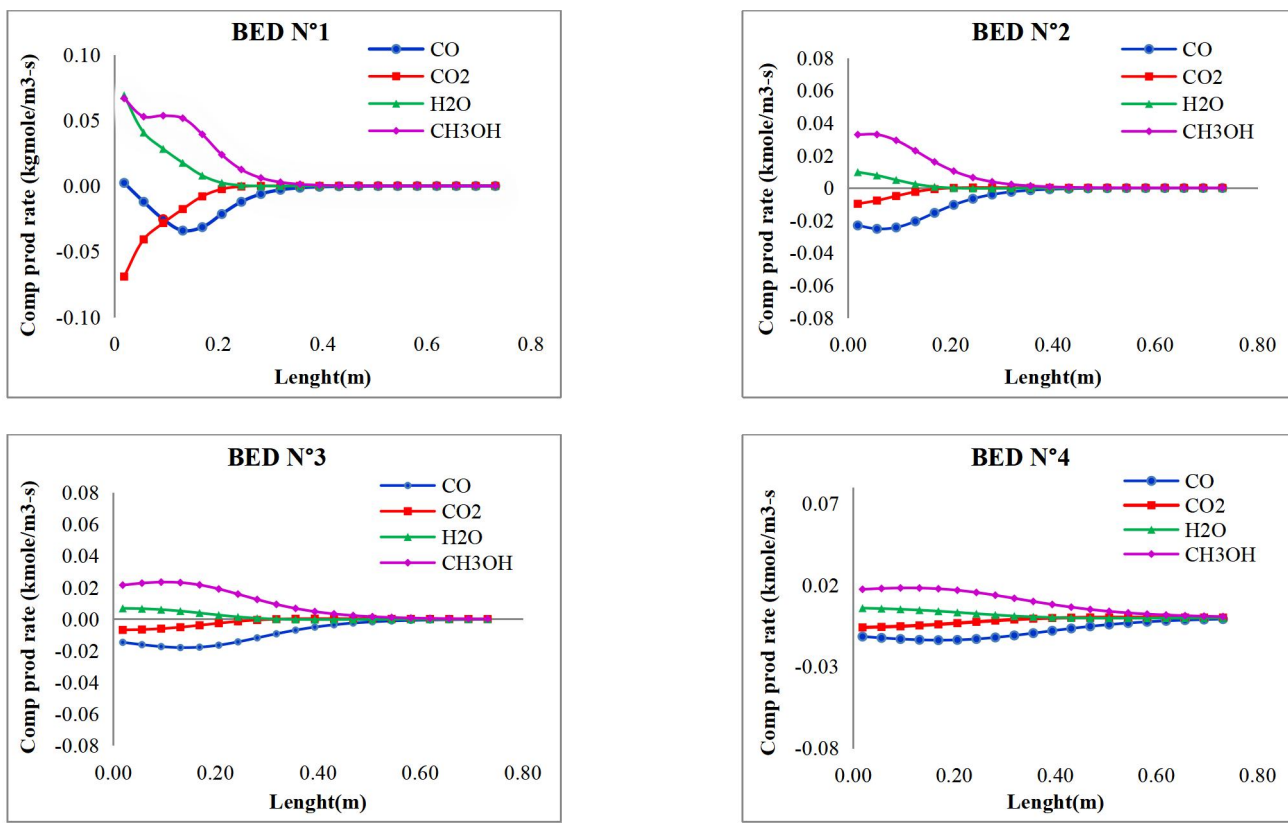


Figure 10—Components Production Rate along the Catalytic Beds.

Results Comparison. We employed identical parameters to those of the Arzew complex in our work, including the molar fraction of reactants at the reactor inlet, flow rate, and operating conditions. The simulation results were then compared with the actual design values.

As shown in **Table 10**, the values obtained using the Aspen-HYSYS software closely resemble the data from the actual reactor, with minor deviations. These differences can be attributed to several factors, including the continuous variation in the flow rate of the cold quench gas, which leads to changes in the component ratios of the gas mixture at the layer level.

Table 10—Comparison of Simulation Results with Real Data.

Composition (Molar fraction %)	Reactor inlet Stream	Reactor Outlet Stream	
		Simulation result	Real data
CH ₄	9.36	9,78	11.20
CO	7.50	5.40	6.80
CO ₂	6.00	7.60	5.74
N ₂	3.26	3.50	3.90
H ₂	73.70	69.35	65.90
H ₂ O	0.13	1.06	1.40
Methanol	0	3.41	3.40

Recycling of Unconverted Gas. Upon analyzing the results of previous simulations, it becomes evident that the production of methanol is limited to approximately 3% due to thermodynamic constraints. This indicates a low conversion rate for the process, with a significant amount of reactants still present in the gas stream exiting the reactor. Research studies have indicated that the average hydrogen conversion rate does not exceed 50% (Timsina et al. 2022).

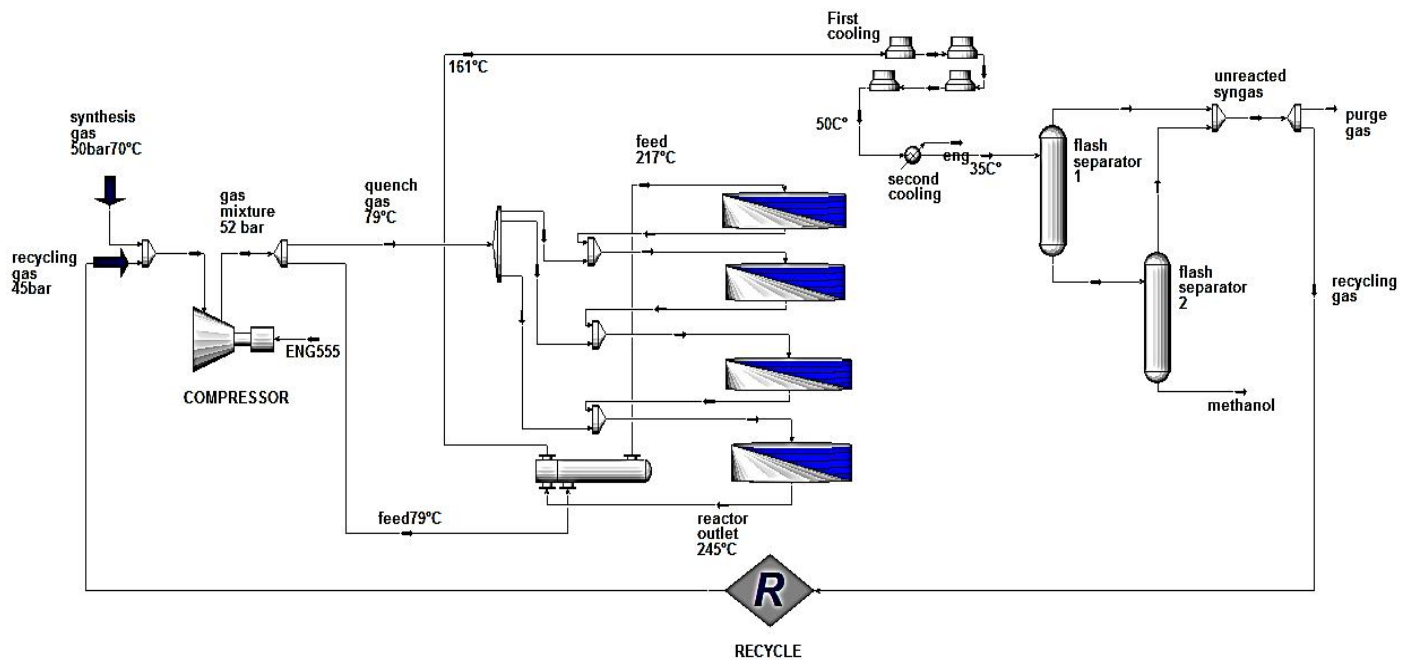


Figure 11—Cycle of methanol process designed in Aspen HYSYS.

Consequently, it is necessary to recover the unconverted syngas for reintegration into the synthesis loop. To enhance performance and efficiency, a flashing process is employed on the methanol reactor stream to separate crude methanol from the unreacted syngas. Approximately 96.5% of the unreacted syngas is then recycled back into the methanol reactor (Arthur 2010).

The remaining portion of the syngas is purged to minimize the accumulation of inert gases such as CH₄ and N₂ within the reaction loop. The accumulation of these gases can have detrimental effects on the reaction

process within the reactor. However, it is important to limit the purging to avoid excessive removal of CO and CO₂ from the inlet stream, as higher purge flow rates result in reduced methanol yields (Abrol and Hilton 2012).

The pressure of the unreacted gas dropped to 43 bars after the flashing operation. Consequently, the mixture is compressed to 52 bars after being combined with the syngas. The recycling loop represents a distinct mathematical process incorporated in Aspen HYSYS (Safari 2022). The calculation of this process follows a sequential modular approach, with iterative conversion of the recycling loops. Thus, it is necessary to recover the unconverted syngas for reintegration into the synthesis loop.

Table 11 presents the methanol production rates obtained from these simulations, both before and after recycling. It is noteworthy that the methanol production rate exhibited a significant increase of 4.1%.

Table 11—Production rates of methanol before and after recycling.

	Before recycling	After recycling
Methanol production flow rate	454,358 k mole/h	547,902 kmole/h
	3.41%.	4.1%

Conclusions

In this research, we investigated the effectiveness of multi-bed reactor simulation through the utilization of plug-flow reactors as a substitute for catalytic layers. Taking the example of an Arzew reactor for methanol synthesis, our study yielded highly consistent results with the actual design data of the Arzew reactor. We obtained a comprehensive understanding of temperature variations within the reactor at each layer's inlet and outlet, enabling precise control of quench gas flow rates. Additionally, we accurately determined the conversion rate of reactants and the percentage of methanol production throughout the reactor.

Furthermore, using Aspen-HYSYS V11 simulation software, we successfully demonstrated the efficiency of using this method to study and control multistage reactors in continuous and discontinuous systems. Therefore, we propose this simple and straightforward approach for the study or control of multi-stage adiabatic reactors for the production of methanol, ammonia, and other products.

Conflict of Interest

The authors declare no conflict of interest

Nomenclature

A	=	frequency factor
a	=	intermolecular forces
B	=	activation energy
b	=	adjusts for molecular size
D_p	=	diameter of particles in the bed, cm
G	=	mass flux, kg/m^2s
g_c	=	conversion factor
K_i^{eq}	=	equilibrium constants
k_i	=	adsorption equilibrium constant for component i
P	=	pressure
P_c	=	critical pressure
P_i	=	partial pressure of component i
R	=	gas constant

- r_i = rate constant for the methanol reaction
 T = temperature
 T_c = critical temperature
 v = molar volume
 Z = length down the packed bed, m
 μ = viscosity of the gas passing through the bed, kg/m.s
 ρ = gas density, kg/m³
 ρ_c = bulk density of the catalyst
 Φ = Porosity, %
 ω = acentric factor
 $(1 - \Phi)$ = the ratio of the volume of solid to the total bed volume

References

- Abate, S., Centi, G., and Perathoner, S. 2015. Chemical Energy Conversion as Enabling Factor to Move to a Renewable Energy Economy. *Green* **5**(6): 43.
- Abrol, S. and Hilton, C. M. 2012. Modeling, Simulation and Advanced Control of Methanol Production from Variable Synthesis Gas Feed. *Computers & Chemical Engineering* **40**:117.
- Adeniyi, A., Eletta, O., and Ighalo, J. O. 2018. Computer Aided Modelling of Low Density Polyethylene Pyrolysis to Produce Synthetic Fuels. *Nigerian Journal of Technology* **37**(4): 945.
- Al-Malah, K. I. 2022. *Aspen Plus: Chemical Engineering Applications*, 2nd edition. Hoboken, New Jersey, USA: John Wiley & Sons.
- Arthur, T. 2010. Control Structure Design for Methanol Process. Master thesis, Norwegian University of Science and Technology, Torgarden, Norway.
- Bendjaouahdou, C. and Bendjaouahdou, M. H. 2014. Control of an Industrial Multi-Staged Catalyst Fixed Bed Reactor. *International Journal of Innovation and Applied Studies* **6**(3): 400.
- Blumberg, T., Morosuk, T., and Tsatsaronis, G. 2017. A Comparative Exergoeconomic Evaluation of the Synthesis Routes for Methanol Production from Natural gas. *Applied Sciences* **7**(12): 1213.
- Bozzano, G. and Manenti, F. 2016. Efficient Methanol Synthesis: Perspectives, Technologies and Optimization Strategies. *Progress in Energy and Combustion Science* **56**: 71-79.
- Bussche, K. V. and Froment, G. F. 1996. A Steady-state Kinetic Model for Methanol Synthesis and the Water Gas Shift Reaction on a Commercial Cu/ZnO/Al₂O₃ Catalyst. *Journal of Catalysis* **1**: 1-10.
- Cui, X. and Kær, S. K. 2020. A Comparative Study on Three Reactor Types for Methanol Synthesis from Syngas and CO₂. *Chemical Engineering Journal* **393**: 124632.
- De Wasch, A. and Froment, G. 1971. A Two Dimensional Heterogeneous Model for Fixed Bed Catalytic Reactors. *Chemical Engineering Science* **26**(5):629-635.
- Elnashaie, S. S. 1994. *Modelling, simulation and optimization of industrial fixed bed catalytic reactors*. Boca Raton, Florida, USA: CRC Press.
- Fossen, M. A., Halvorsrød, J., Narvestad, T., et al. 2022. ASPEN HYSYS Simulation of the Methanol Synthesis Based on Gas from Biomass Gasification. Paper presented at the 63rd International Conference of Scandinavian Simulation Society, Trondheim, Norway, 20-21 September.
- Froment, G. 1972. Analysis and design of fixed bed catalytic reactors: Chapter 1pp 1-55. ACS Publications.
- Fuad, M. N., Hussain, M. A., and Zakaria, A. 2012. Optimization Strategy for Long-Term Catalyst Deactivation in a Fixed-Bed Reactor for Methanol Synthesis Process. *Computers & Chemical Engineering* **44**: 104-126.
- Goeppert, A., Czaun, M., Jones, J.P., et al. 2014. Recycling of Carbon Dioxide to Methanol and Derived Products-Closing the Loop. *Chemical Society Reviews* **43**(23): 7995.
- Graaf, G. H., Sijtsema, P. J. J. M., Stamhuis, E. J., et al. 1986. Chemical Equilibria in Methanol Synthesis. *Chemical Engineering Science* **41**(11): 2883-2890.
- Graaf, G. H., Scholtens, H., Stamhuis, E. J., et al. 1990. Intra-particle Diffusion Limitations in Low-Pressure Methanol Synthesis. *Chemical Engineering Science* **45**(4): 773-783.

- Grabow, L. and Mavrikakis, M. 2011. Mechanism of Methanol Synthesis on Cu through CO₂ and CO Hydrogenation. *Acs Catalysis* **1**(4): 365.
- HYSYS, Version 11. 2004. Burlington, MA, USA: Aspen Technology.
- Lee, S. 1989. *Methanol Synthesis Technology*. Boca Raton, Florida, USA: CRC Press.
- Liu, Z. and Karimi, I. A. 2018. Simulating Combined Cycle Gas Turbine Power Plants in Aspen HYSYS. *Energy Conversion and Management* **171**: 1213.
- Løvik, I. 2001. Modelling, Estimation and Optimization of the Methanol Synthesis with Catalyst Deactivation. PhD dissertation, Norwegian University of Science and Technology, Torgarden, Norway.
- Moulijn, J. A., Makkee, M., and Van Diepen, A. E. 2013. *Chemical process technology*. Hoboken, New Jersey, USA: John Wiley & Sons.
- Nestler, F., Krüger, M., Full, J., et al. 2018. Methanol Synthesis–Industrial Challenges Within a Changing Raw Material Landscape. *Chemie Ingenieur Technik* **90**(10): 1409-1418.
- Ortiz, F. G., Serrera, A., Galera, S., et al. 2013. Methanol synthesis from syngas obtained by supercritical water reforming of glycerol. *Fuel*, 105: 739.
- Safari, A. 2022. Automation of control degrees of freedom in Aspen Hysys. *IFAC Journal of Systems and Control* **19**: 100187.
- Shi, C., Labbaf, B., Mostafavi, E., et al. 2020. Methanol Production from Water Electrolysis and Tri-Reforming: Process Design and Technical-Economic Analysis. *Journal of CO2 Utilization* **38**: 241.
- Sinadinovic-Fiser, S., Jankovic, M., and Radicevic, R. 2001. Simulation of the Fixed-Bed Reactor for Methanol Synthesis. *Petroleum and Coal* **43**(1): 31.
- Skrzypek, J., Lachowska, M., Grzesik, M., et al. 1995. Thermodynamics and Kinetics of Low Pressure Methanol Synthesis. *The Chemical Engineering Journal and the Biochemical Engineering Journal* **58**(2): 101.
- Slattery, J. C. 1972. *Momentum, Energy, and Mass Transfer in Continua*. New York, USA: McGraw-Hill Book Co.
- Timsina, R., Thapa, R. K., Moldestad, B. M., et al. 2022. Methanol Synthesis from Syngas: A Process Simulation. Paper presented at the 62nd International Conference of Scandinavian Simulation Society, Virtual, Finland, 21-23 September.
- Towler, G. and Sinnott, R. 2022. *Chemical Engineering Design (Third Edition)*. Berkeley, CA, USA: Elsevier Ltd.
- Tripodi, A., Compagnoni, M., Martinazzo, R., et al. 2017. Kinetic Modelling at the Basis of Process Simulation for Heterogeneous Catalytic Process Design. <https://europepmc.org/article/PPR/PPR53039>.(accessed 17 May 2023).
- Varma, A. 1981. Packed Bed Reactors Chemical Reactors. *American Chemical Society* **168**:279-286.
- Waugh, K. C. 2012. Methanol Synthesis. *Catalysis Letters* **142**(10): 1153-1166.

Sidi-yacoub Ilhem, a Ph.D. candidate in Process Engineering Department, Faculty of Science and Technology, Abdelhamid Ibn Badis University, (UMAB), Algeria. Ilhem holds a master's in Chemistry. His specializes in Materials Elaboration and Valorization.

Ahmed Feddag, is the Professor in Process Engineering Department of Abdelhamid Ibn Badis University (UMAB), Algeria.

Khelifa Ikram, is a Ph.D in Process Engineering, Djillali Liabes University, Sidi Bel Abbès, Algeria. He is a Process Engineer at Study and Development Department-GL3Z Gas Liquefaction Complex, Algeria.